

Full experimental modelling of a liver tissue mimicking phantom for medical ultrasound studies employing different hydrogels

Sergio Casciaro · Francesco Conversano ·
Stefano Musio · Ernesto Casciaro ·
Christian Demitri · Alessandro Sannino

Received: 5 August 2008 / Accepted: 3 November 2008 / Published online: 4 December 2008
© Springer Science+Business Media, LLC 2008

Abstract Tissue mimicking phantoms have been widely reported to be an important tool for development, optimisation and performance testing of ultrasound-based diagnostic techniques. In particular, modern applications of tissue mimicking phantoms often include characterisation of the nonlinear behaviour of experimental ultrasound contrast agents. In such cases, the tissue-mimicking materials should be chosen not only based on the values of their density, speed of sound and attenuation coefficient, but also considering their effect on the appearance of “native harmonics” due to nonlinear distortion of ultrasound signal during propagation. In a previous paper it was demonstrated that a cellulose-based hydrogel is suitable to simulate nonlinear acoustical behaviour of liver tissue for thicknesses up to 8 cm. In this paper we present the experimental characterisation of the nonlinear acoustical behaviour of a different polyethylene glycol diacrylate (PEGDA)-based hydrogel, in order to assess whether and how it can improve the performances and overcome some limitations of the cellulose-based hydrogel as liver tissue-mimicking material. Samples of pig liver tissue, cellulose-based hydrogel and PEGDA-based hydrogel were insonified in a through-transmission set-up, employing 2.25-MHz pulses with different mechanical

index (MI) values. Second harmonic and first harmonic amplitudes were extracted from the spectra of received signals and their difference was then used to compare sample behaviours. Obtained results show how a new more accurate and combined experimental model of linear and nonlinear acoustical behaviour of liver tissue is feasible. In fact, a further confirmation of the cellulose-based hydrogel effectiveness to precisely simulate the liver tissue for penetration depths up to 8 cm was provided, and it was also shown that the employment of the PEGDA-based hydrogel can extend the range of useful tissue-mimicking material thicknesses up to 11 cm, moreover allowing a considerable improvement of the time stability and behaviour reliability of the corresponding manufactured phantoms.

1 Introduction

Contrast agents for ultrasound (US) imaging are currently used for several clinical applications, such as blood signal enhancement [1], myocardial perfusion imaging [2] and characterisation of liver lesions [3].

In very recent years, research in targeted microbubble contrast agents and the initial development of smaller nanoparticle-based agents for US imaging have opened new exciting perspectives in this field [4, 5]: ultrasound molecular imaging (which relies on the detection of disease-targeted contrast particles), effective combination of echography with other non-invasive imaging techniques to perform multimodal diagnostic studies, novel therapeutic strategies based on the site-targeted delivery of drugs and/or genes.

In order to reach these goals, however, an ever greater and deeper understanding of the relationships between

S. Casciaro (✉) · F. Conversano · S. Musio · E. Casciaro
Institute of Clinical Physiology, National Council of Research
(IFC-CNR), c/o Campus Ecotekne, via per Monteroni,
73100 Lecce, Italy
e-mail: casciaro@ifc.cnr.it

S. Casciaro · F. Conversano · S. Musio · E. Casciaro
Bioengineering Division, Euro Mediterranean Scientific
Biomedical Institute, Brindisi, Italy

C. Demitri · A. Sannino
Department of Engineering for Innovation,
University of Salento, Lecce, Italy

transmitted US parameters and contrast agent behaviour is required [6], implying the need for reliable *in vitro* systems capable of accurately reproducing acoustic properties and anatomical configurations of human organs.

Tissue-mimicking phantoms have been widely reported to be an important tool for development, optimisation and performance testing of ultrasound-based diagnostic techniques [7–14]. Some examples of commonly employed tissue-mimicking materials are polyvinyl alcohol (PVA) [15, 16], polyacrylamide (PAA) [17–19], gelatine [20, 21], agar [22] and silicone [23].

In particular, it has been recently shown that different kinds of hydrogels can be efficiently used for phantom design [7–9]. In fact, hydrogels are hydrophilic cross-linked polymers which are expanded in water and possess properties that make them attractive for biomedical applications: they have low acoustic attenuation and their acoustic impedance and speed of sound can be modulated to be very close to biological tissue values, furthermore they generally can be shaped into arbitrary solid structures [7].

However, modern applications of tissue-mimicking phantoms often include characterisation of the nonlinear behaviour of experimental US contrast agents, which introduces in the scattered US signal specific harmonic components that are then exploited to produce echographic images in various harmonic modalities [24, 25]. In such cases, there is in principle the possibility of confusing actual contrast agent harmonics with those generated by nonlinear distortion of ultrasound during its propagation (native harmonics). Therefore, as it has been pointed out in a previous paper [9], materials to be employed in the manufacturing of tissue-mimicking phantoms should be chosen not only based on the values of their density, speed of sound and attenuation coefficient, but also considering their effect on the appearance of native harmonics during ultrasound propagation through them. In our previous work [9] we demonstrated that a cellulose-based hydrogel is a very suitable candidate to simulate linear and nonlinear US propagation in liver tissue for penetration depths up to 8 cm.

In this paper we present the experimental characterisation of the nonlinear acoustical behaviour of a different polyethylene glycol diacrylate (PEGDA)-based hydrogel, in order to assess, through direct comparison with measurements performed on both the cellulose-based hydrogel and the reference biological tissue, whether the acrylic PEGDA-based hydrogel can improve the performances of the cellulose-based hydrogel as liver tissue-mimicking material, regarding the accuracy in nonlinear behaviour simulation, the effectively employable material thickness and the duration of the correspondingly manufactured phantom. The final goal of these research studies is the achievement of a fully characterised experimental model for *in vitro* simulation of liver tissue acoustical behaviour.

2 Materials and methods

2.1 PEGDA-based hydrogel

PEGDA (purchased from Sigma-Aldrich, Milano, Italy) is a bifunctional molecule (molecular weight 700) that can be polymerised by means of free radicals deriving from the decomposition of appropriate photoinitiators. PEGDA-based hydrogel samples were obtained starting from a water solution of polymer and photoinitiator (Darocur 1173[®], Ciba Specialty Chemicals, Milano, Italy). This solution was prepared by first dissolving the photoinitiator in PEGDA by gently stirring at room temperature until a homogeneous mixture was obtained (photoinitiator concentration was 2% w/v polymer), then distilled water was slowly added up to reach 15% w/v of polymer in water. The crosslinking reaction started when the samples were placed under an UV lamp (340 nm).

A preliminary acoustical characterisation of this hydrogel was presented in a recent paper by our research group [8], showing in particular that the synthesized hydrogel has values of speed of sound and acoustic impedance very close to those reported in literature for liver tissue [26].

2.2 Cellulose-based hydrogel and pig liver

A cellulose-based hydrogel [9] was synthesized by cross-linking water solutions of carboxymethylcellulose sodium salt (CMCNa) and hydroxyethylcellulose (HEC), using divinylsulfone (DVS) as a crosslinking agent. After the mixing stage, an alkaline water solution of potassium hydroxide (KOH) was added as a catalyst and hydrogel formation occurred at room temperature after 12–14 h.

In this case, the total polymer weight fraction in the solution was 2%, with a fixed CMCNa/HEC weight ratio of 1.5/1, because we demonstrated [8] that this value assures the achievement of a hydrogel with acoustic impedance and attenuation coefficient very close to those of the reference liver tissue.

Pig liver was selected as the reference tissue for its properties very similar to human liver [27]. The samples to investigate were excised a few minutes before measurements, immediately after slaughter, and kept at room temperature. These tissue samples were used to compare their harmonic behaviour with the corresponding ones of the synthesized hydrogels.

2.3 Experimental setup and measurement procedure

A scheme of the adopted experimental apparatus [9] is reported in Fig. 1 and its essential features are summarised herein.

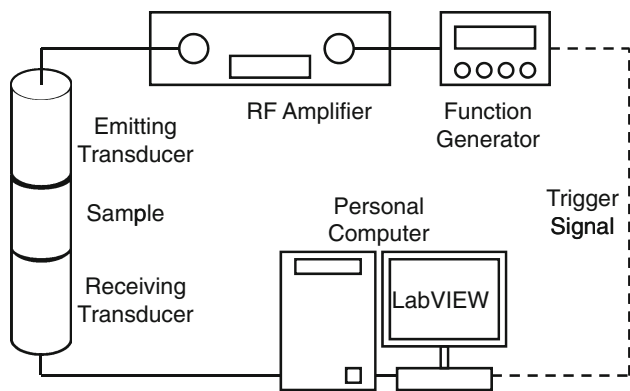


Fig. 1 Scheme of the experimental setup. Signals generated by the function generator were first amplified in the RF amplifier and then supplied to the emitting transducer; signals transmitted through the sample reached the receiving transducer, connected to the personal computer that digitized and stored the received signals. Function generator trigger and data transfer were controlled by a virtual instrument realised with LabViewTM (National Instruments Corporation, Austin, TX)

A programmable function generator (TG1010A, Thurlby Thandar Instruments Ltd., Huntingdon, U.K.) provided the generation of 2.25-MHz 10-cycle pulses with a pulse repetition frequency (PRF) of 10 Hz. These signals were first amplified in a radiofrequency (RF) power amplifier (FLL-75, Frankonia MV-Mess-Systeme GmbH, Heideck, Germany) and then supplied to a 2.25-MHz US transducer (V306, Panametrics, Olympus NDT, Waltam, MA). Signals transmitted through the samples were received by a 3.5-MHz US transducer (V382, Panametrics, Olympus NDT, Waltam, MA), that was connected to a computer *via* a data-acquisition board (PCI-5122, National Instruments Corporation, Austin, TX) used to digitize (100 MHz, 14 bits) the signals, that were then stored in the computer hard disk for off-line analysis. The function generator and the data transfer were controlled by a virtual instrument realised with LabViewTM (National Instruments Corporation, Austin, TX). The same software was also employed to implement the needed algorithms for off-line data analysis.

These measurements were carried out to compare the onset of native harmonics in the PEGDA-based hydrogel with the corresponding in pig liver and cellulose-based hydrogel for different mechanical index (MI) values and sample thicknesses, aiming to find the best liver tissue mimicking material for each couple of chosen parameter values. MI is related to the acoustic pressure according to the equation $MI = Pa/f^{1/2}$, where Pa represents the absolute value of negative acoustic pressure peak measured in the matter and f is the ultrasound frequency. (Further details on MI and its measurement are available in our previous paper [9]).

In particular, we focused on the appearance of second harmonic, that was evaluated through the computation of

the difference ($H_2 - H_1$), expressed in decibels, where H_1 and H_2 represent respectively first harmonic and second harmonic amplitude extracted from the received signal spectra.

For each of the three tested materials (pig liver tissue, cellulose-based hydrogel and PEGDA-based hydrogel), we insonified samples of seven different thicknesses (range 5–11 cm) employing six different MI values (range 0.1–0.6), so a total of 42 combinations of tissue thickness and incident ultrasound amplitude were investigated.

The digitized signals were processed using a LabViewTM custom designed software tool, that performed the correction of the acquired signal spectra to take into account the receiver characteristics (spectral correction was based on the broadband FFT spectrum of the probe [28]) and, from each corrected spectrum, calculated the quantity ($H_2 - H_1$). Obtained results were then averaged over sequences of 30 signals, consecutively acquired in the same conditions, and plotted both as a function of sample thickness (i.e., penetration depth) and as a function of MI value (i.e., ultrasound amplitude).

3 Results and discussion

Nonlinear propagation effects of diagnostic ultrasound were investigated in pig liver tissue and in two different hydrogels for tissue mimicking purposes: a cellulose-based hydrogel recently demonstrated to be a very suitable candidate to simulate the nonlinear US propagation in liver tissue for penetration depths up to 8 cm [9] and a new PEGDA-based hydrogel that, to our knowledge, had been never used for in vitro simulation of biological tissue behaviour.

In particular, we employed narrowband US pulses at the frequency of 2.25 MHz and the nonlinear signal distortion during propagation (i.e., the appearance of native harmonics) was quantified by the difference ($H_2 - H_1$), computed on the received signal spectra. Effects of incident ultrasound amplitude and penetration depth were separately assessed by insonifying samples of variable thickness (5–11 cm) with different MI values (0.1–0.6).

Figure 2a shows the obtained plots of ($H_2 - H_1$) against distance for the three tested materials in the case of $MI = 0.1$. Each sample shows a nonlinear behaviour confirming what was described in [9]: native harmonic generation initially increases with penetration depth until its maximum, after which it shows a drop, reasonably due to the appearance of higher harmonics. In this specific case, all the reported curves reach their peak in correspondence of a sample thickness of 9 cm, but their shapes are quite different, producing the visible consequence that liver behaviour is better approximated by the cellulose-based

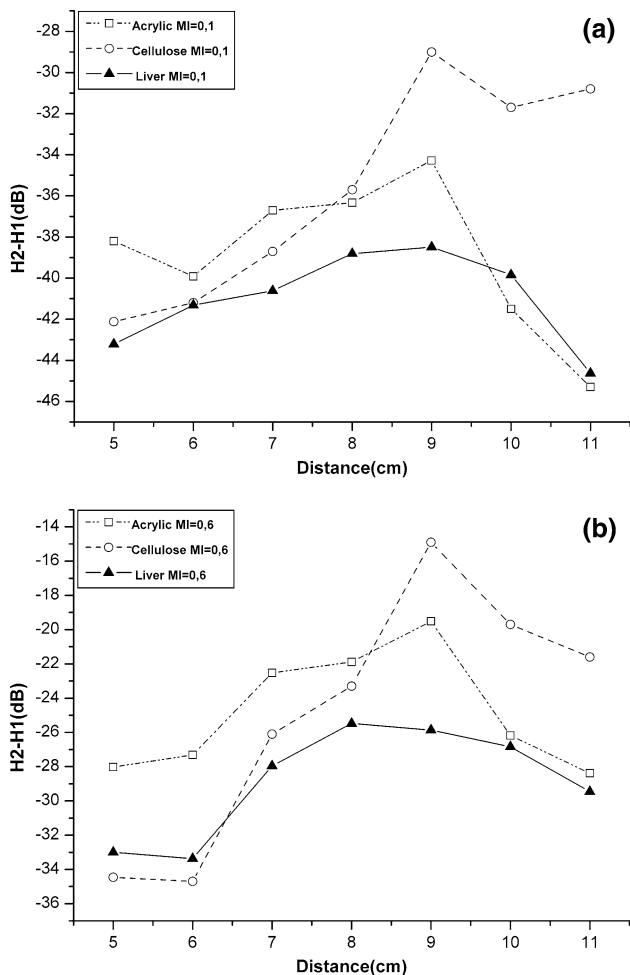


Fig. 2 Plot of measured (H_2-H_1) values for liver, cellulose-based hydrogel and acrylic (PEGDA-based) hydrogel against sample thickness (10-cycle pulses; 2.25-MHz US frequency; PRF = 10 Hz): **a** MI = 0.1, **b** MI = 0.6. Liver behaviour is better approximated by the cellulose-based hydrogel for penetration depths lower than 8 cm, while for the thicker samples the acrylic hydrogel becomes the most suitable choice, independently of the employed MI

hydrogel for penetration depths lower than 8 cm, while for thicker samples the acrylic hydrogel becomes the best in mimicking nonlinear ultrasound distortion in the reference biological tissue.

This is due to the fact that, for each material, the shape of the corresponding reported curve is mainly governed by two factors: internal microstructure and attenuation coefficient. Material microstructure is directly responsible for US signal distortion during propagation, which results in appearance of harmonic components at higher frequencies. These harmonics are then attenuated more rapidly than the fundamental component at the transmitted frequency, because the attenuation coefficient always increases with frequency [29]. Therefore, for each penetration depth, the difference (H_2-H_1) is the result of a complex balance between the amount of second harmonic generated by

nonlinear signal distortion (depending on material microstructure) and the quantity of fundamental component and second harmonic component that have been attenuated at the considered depth (both determined by attenuation coefficient). Moreover, when signal distortion reaches a certain level, further nonlinearity introduction does not augment anymore the second harmonic intensity, but causes the appearance of higher order harmonics. Hence, from this point on, second harmonic production is no more increased while it continues to be attenuated, so explaining the drop of (H_2-H_1) showed by each curve after the peak.

In order to summarise the discussed concepts, for each curve reported in Fig. 2a, we can say that in the “low-depth” part the second harmonic generation due to progressive signal distortion compensates for simultaneous attenuation, resulting in an increasing value of (H_2-H_1) , while after the peak second harmonic production is taken over by attenuation phenomena and generation of higher harmonics, giving the decreasing trend observed in the final part of the curves.

Taking into account these considerations, the specific trends showed in Fig. 2a by all the studied materials can be explained in the following way. Considering liver tissue and cellulose-based hydrogel, we know [8] that their attenuation coefficients are very similar, but the hydrogel microstructure is probably more distorting, so resulting in two curves that are very close for the lower penetration depths, but then progressively move away from each other as a consequence of different microstructures. On the other hand, acrylic hydrogel has a more distorting internal structure (in fact low sample thicknesses cause higher harmonic generation with respect to the other materials), but the attenuation coefficient is also slightly higher, resulting in a smaller slope of the growing tract of the curve. This is emphasised also by the marked drop observed in the last part, where the effect of attenuation overtakes second harmonic production.

The discussed behaviour was confirmed for all the employed MI values. As an example, the curves obtained with MI = 0.6 are reported in Fig. 2b.

The results obtained when using 8-cm thick samples require further comments. In fact, in correspondence of this specific penetration depth, in Fig. 2a (MI = 0.1) acrylic hydrogel curve is the closest to the liver one, but in Fig. 2b (MI = 0.6) cellulose-based hydrogel is the best simulator of liver behaviour at same depth. In order to clarify this, we plotted in Fig. 3 the values of (H_2-H_1) measured on the 8-cm thick samples as a function of MI. From the reported curves it is evident that cellulose-based hydrogel is the best in simulating nonlinear US distortion in liver for the considered penetration depth. In fact, for five out of six tested MI, the value of (H_2-H_1) measured in the cellulose-based hydrogel is clearly closer to the liver one than the

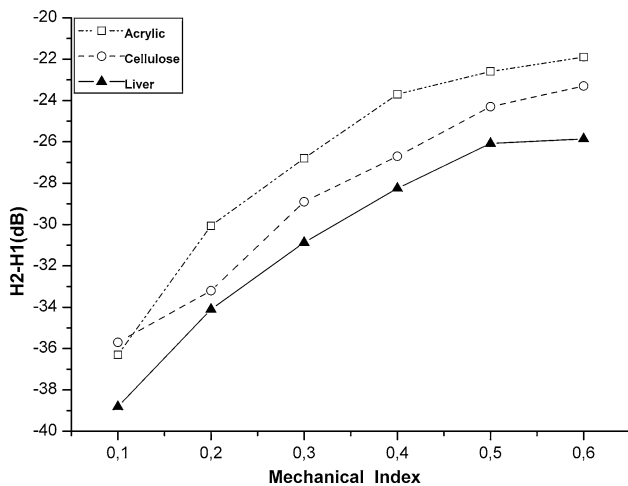


Fig. 3 Plot of measured (H2–H1) values for liver, cellulose-based hydrogel and acrylic (PEGDA-based) hydrogel against MI value (8-cm sample thickness; 10-cycle pulses; 2.25-MHz US frequency; PRF = 10 Hz). The behaviours of the two hydrogels are almost equivalent at MI = 0.1, but for higher acoustic pressures the cellulose-based hydrogel is definitely better than the acrylic one in mimicking ultrasound propagation in liver tissue

corresponding measured in the acrylic hydrogel. The only exception is represented by the points referring to MI = 0.1, but in this case, given the low signal amplitude, the measurements are intrinsically more affected by the noise and the values of the two hydrogels are also very close to each other. Therefore, we can conclude that the behaviours of the two hydrogels for 8-cm penetration depth are equivalent at MI = 0.1, but for higher ultrasound intensities cellulose-based hydrogel is better than the acrylic one in mimicking nonlinear US distortion in liver tissue, and this is clearly visible already for MI = 0.2, as additionally proved by the curves plotted in Fig. 4 (MI = 0.2, variable sample thickness).

These findings represent a further confirmation of the results we published in our previous work [9], in which we stated that cellulose-based hydrogel is a very suitable candidate to in vitro simulate the nonlinear ultrasound propagation in liver tissue for penetration depths up to 8 cm.

Moreover, the results of present study further extend the range of liver tissue modelling of thicknesses whose nonlinear acoustical behaviour can be effectively simulated through the employment of tissue-mimicking hydrogels. In fact, besides the confirmed effectiveness of our cellulose-based hydrogel for penetration depths up to 8 cm, we showed how the use of a specific PEGDA-based hydrogel is capable of successfully reproducing native harmonic generation in liver tissue for penetration depths in the range 8–11 cm.

In order to provide an additional visual evidence of our findings, we reported in Fig. 5a the curves of nonlinear signal distortion for the three tested materials as a function

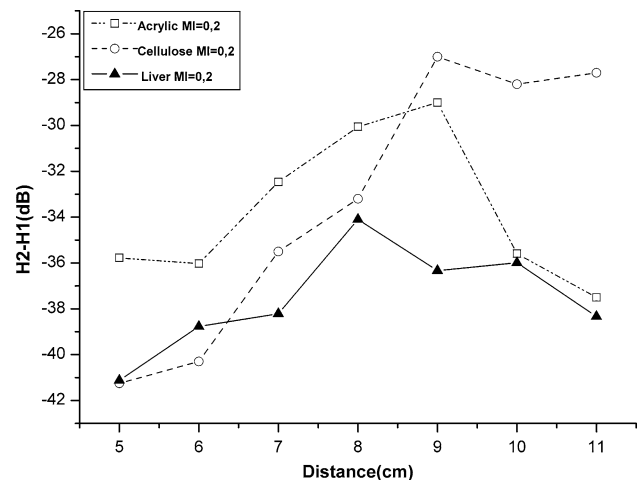


Fig. 4 Plot of measured (H2–H1) values for liver, cellulose-based hydrogel and acrylic (PEGDA-based) hydrogel against sample thickness (MI = 0.2; 10-cycle pulses; 2.25-MHz US frequency; PRF = 10 Hz). Reported curves further confirm that the cellulose-based hydrogel is the most suitable candidate to simulate nonlinear behaviour of liver tissue for penetration depths up to 8 cm

of MI for the 6-cm sample thickness, while in Fig. 5b we plotted the corresponding curves obtained for the 10-cm sample thickness. In the first case (Fig. 5a), the chosen penetration depth belongs to the range in which the cellulose-based hydrogel is the best choice, and in fact its curve is almost coincident with that of liver tissue while the corresponding values measured in PEGDA-based hydrogel are always higher. In the second case (Fig. 5b), the situation is inverted: 10-cm penetration depth is one of the typical values for which the employment of the acrylic hydrogel is the most suitable choice, and this is again proved by the substantial superimposition of the corresponding curve to the liver one, while the curve of cellulose-based hydrogel always presents higher values.

The discussed results represent an extension of previously known experimental models of liver tissue acoustical behaviour and they have also important implications for the practical employment of hydrogels in the manufacturing of tissue-mimicking phantoms. In fact, both the synthetic materials we tested can be cast into arbitrary shapes and are suitable to produce tissue-mimicking phantoms (in the case of acrylic hydrogel it is further required the use of a mould which is transparent to UV rays, to allow the crosslinking reaction), but the duration of the obtained products is significantly different: a phantom containing the cellulose-based hydrogel requires to be stored in a closed box in refrigerator, assuring high moisture, and it can then be used for 4 weeks [8], while a phantom based on the acrylic hydrogel can be used for more than 1 year, provided that it is stored in a water bath inside a refrigerator.

Currently, we are already working to further extend the potential and practical usefulness of this kind of tissue-

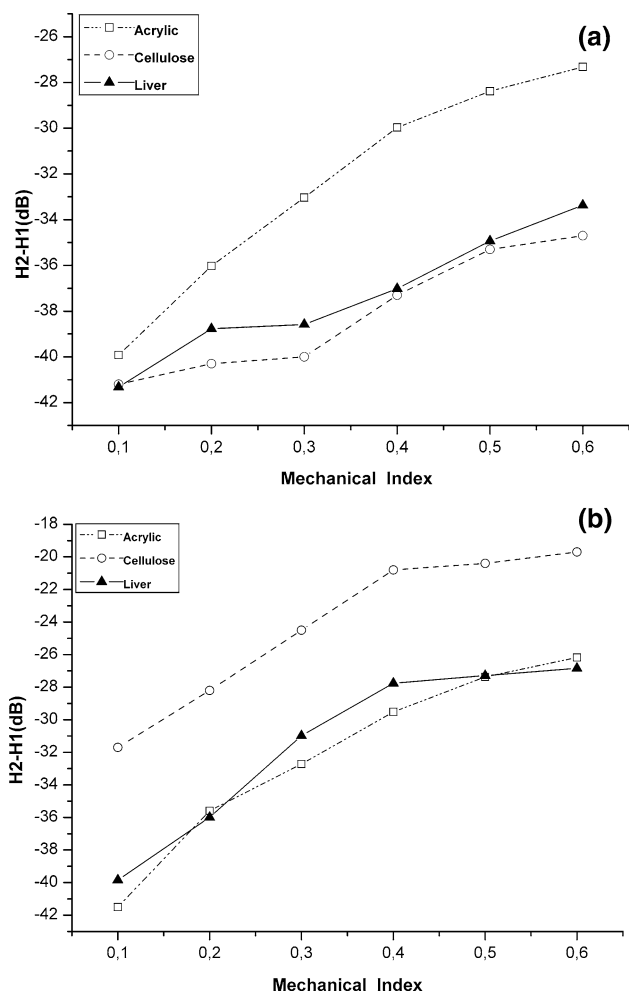


Fig. 5 Plot of measured (H2–H1) values for liver, cellulose-based hydrogel and acrylic (PEGDA-based) hydrogel against MI value (10-cycle pulses; 2.25-MHz US frequency; PRF = 10 Hz): **a** 6-cm sample thickness, **b** 10-cm sample thickness. In the case of 6-cm penetration depth, the cellulose-based hydrogel is clearly the best choice to simulate liver behaviour, while for a 10-cm depth the situation is inverted and the acrylic hydrogel is better

mimicking phantoms. In particular, we recently published [8] the experimental results of a first employment of these hydrogels in the manufacturing of a liver-mimicking phantom for in vitro characterisation of experimental ultrasound contrast agents. In the cited paper we presented an innovative experimental setup in which one of our phantoms was inserted in a fluidodynamic circuit allowing contrast agent studies in different flow conditions (in that specific case modifiable by acting on a peristaltic pump).

Ongoing work includes the simulation of pathological events in our artificial tissues, achievable, for example, by realising a mass of a given shape employing a different hydrogel, characterised to have mechanical and acoustic properties close to those of a specific tumour. This separately manufactured mass will be included in the hydrogel before crosslinking reaction takes place, in order to stay

“trapped” in a pre-determined position in the final phantom. The same technique could be also employed to simulate different tissue structures of an healthy organ. In principle, the same result could be also obtained by simply varying the concentration of the zonal reagents.

A further step will be represented by the employment of a three-dimensional stereolithographic technique on PEGDA-based hydrogels, in order to obtain more accurate geometric reproductions of anatomical structures and more complex and realistic flow conditions, both normal and pathological. Among the possible future uses of such realistic phantoms, we can mention the efficacy test of innovative image processing algorithms, dedicated, for example, to non-invasive tumour characterisation or to automatic segmentation of complex vessel structures for accurate surgery planning.

4 Conclusions

This study investigated nonlinear propagation effects of diagnostic ultrasound in pig liver tissue and in two different hydrogels for tissue mimicking purposes: a cellulose-based hydrogel and an acrylic PEGDA-based hydrogel. The former had been recently demonstrated to be very suitable to simulate the nonlinear ultrasound propagation in liver tissue for penetration depths up to 8 cm, and so it was used as a comparison term to assess the potential of the latter for improving the performances of currently available liver tissue-mimicking phantoms. The onset of native harmonics in all the materials was studied independently as a function of the incident MI and of the penetration depth.

Presented results provided a further confirmation of the actual effectiveness of the cellulose-based hydrogel to precisely simulate the liver tissue acoustical behaviour for penetration depths up to 8 cm, but it was also showed how the acrylic hydrogel employment can extend the range of useful tissue-mimicking material thicknesses up to 11 cm. In this way researchers are allowed to in vitro reproduce the conditions of deeper liver vessels, without losing accuracy in the laboratory recreation of the specific local environment. Therefore, the combination of the two hydrogels we synthesized and characterised constitutes a new experimental model of liver tissue acoustical behaviour, through which it is possible the accurate simulation of linear and nonlinear acoustic response of this biological tissue on a wide range of depths.

Furthermore, the employment of the PEGDA-based hydrogel for tissue-mimicking purposes will considerably lengthen the duration of the corresponding manufactured phantoms from a few weeks (achievable with cellulose-based hydrogel) to more than 1 year, so facilitating the repetition of experimental studies with reliable boundary conditions.

Finally, a reasonable future perspective of this research field is the employment of a three-dimensional stereolithographic technique on PEGDA-based hydrogels, that will ensure a marked increase in geometric accuracy of the obtained phantoms thanks to shape reproduction very close to the real human liver, exploiting the information available from clinical studies of the liver with high resolution imaging techniques.

Acknowledgments This work was partially funded by the MUR Project DM18640 (Rif. Min. DD MIUR 14.5.2005 n.602/Ric/2005), granted by the Italian Ministry of Research, and the ARIS*ER Project (Marie Curie Research Training Network MRTN-CT-2004-512400) granted by EU.

References

1. D.W. Droste, *Eur. Neurol.* **59**(Suppl. 1), 2 (2008). doi: [10.1159/000114454](https://doi.org/10.1159/000114454)
2. D.J. Rakhit, H. Becher, M. Monaghan, P. Nihoyannopoulos, R. Senior, *Eur. J. Echocardiogr.* **8**, S24 (2007). doi: [10.1016/j.euje.2007.03.005](https://doi.org/10.1016/j.euje.2007.03.005)
3. R. Lencioni, C. Della Pina, L. Crocetti, E. Bozzi, D. Cioni, *Eur. Radiol.* **17**(Suppl. 6), F73 (2007)
4. F. Conversano, S. Casciaro, in *New Technology Frontiers in Minimally Invasive Therapies*, ed. by S. Casciaro, B. Gersak (Lupiensis Biomedical Publications, Lecce, Italy, 2007), p. 161
5. S. Casciaro, F. Conversano, in *Minimally Invasive Technologies and Nanosystems for Diagnosis and Therapies*, ed. by S. Casciaro, E. Samset (Lupiensis Biomedical Publications, Lecce, Italy, 2008), p. 113
6. S. Casciaro, R. Palmizio Errico, F. Conversano, C. Demitri, A. Distante, *Invest. Radiol.* **42**, 95 (2007). doi: [10.1097/01.rli.0000251576.68097.d1](https://doi.org/10.1097/01.rli.0000251576.68097.d1)
7. K. Zell, J.I. Sperl, M.W. Vogel, R. Niessner, C. Haisch, *Phys. Med. Biol.* **52**, N475 (2007). doi: [10.1088/0031-9155/52/20/N02](https://doi.org/10.1088/0031-9155/52/20/N02)
8. C. Demitri, A. Sannino, F. Conversano, S. Casciaro, A. Distante, A. Maffezzoli, *J. Biomed. Mater. Res. Part B*. Published online June 5, (2008)
9. S. Casciaro, C. Demitri, F. Conversano, E. Casciaro, A. Distante, *J. Mater. Sci.: Mater. Med.* **19**, 899 (2008). doi: [10.1007/s10856-007-3007-8](https://doi.org/10.1007/s10856-007-3007-8)
10. B.S. John, D. Rowland, L. Ratnam, M. Walkden, S. Nayak, U. Patel, K. Anson, D. Nassiri, *Ultrasound Med. Biol.* Published online May 14, (2008)
11. R.S. Singh, M.O. Culjat, W.S. Grundfest, E.R. Brown, S.N. White, *J. Acoust. Soc. Am.* **123**, EL39 (2008). doi: [10.1121/1.2884083](https://doi.org/10.1121/1.2884083)
12. H.-L. Liu, Y.-Y. Chen, W.-S. Chen, T.-C. Shih, J.-S. Chen, W.-L. Lin, *Ultrasound Med. Biol.* **32**, 1411 (2006). doi: [10.1016/j.ultrasmedbio.2006.05.008](https://doi.org/10.1016/j.ultrasmedbio.2006.05.008)
13. C.M. Moran, T. Anderson, S.D. Pye, V. Sboros, W.N. McDicken, *Ultrasound Med. Biol.* **26**, 629 (2000). doi: [10.1016/S0301-5629\(00\)00148-4](https://doi.org/10.1016/S0301-5629(00)00148-4)
14. C.J.P.M. Teirlinck, R.A. Bezemer, C. Kollmann, J. Lubbers, P.R. Hoskins, P. Fish, K.-E. Fredfeldt, U.G. Schaarschmidt, *Ultrasonics* **36**, 653 (1998). doi: [10.1016/S0041-624X\(97\)00150-9](https://doi.org/10.1016/S0041-624X(97)00150-9)
15. S. Manohar, A. Kharine, J.C.G. Van Hespren, W. Steenbergen, T.G. Van Leeuwen, *J. Biomed. Opt.* **9**, 1172 (2004). doi: [10.1117/1.1803548](https://doi.org/10.1117/1.1803548)
16. A. Kharine, S. Manohar, R. Seeton, G.M. Kolkman Roy, A. Bolt Rene, W. Steenbergen, F.M. De Mul Frits, *Phys. Med. Biol.* **48**, 357 (2003). doi: [10.1088/0031-9155/48/3/306](https://doi.org/10.1088/0031-9155/48/3/306)
17. K. Takegami, Y. Kaneko, T. Watanabe, T. Maruyama, Y. Matsumoto, H. Nagawa, *Ultrasound Med. Biol.* **30**, 1419 (2004). doi: [10.1016/j.ultrasmedbio.2004.07.016](https://doi.org/10.1016/j.ultrasmedbio.2004.07.016)
18. C. Lafon, V. Zderic, M.L. Noble, J.C. Yuen, P.J. Kaczkowski, O.A. Sapozhnikov, F. Chavier, L.A. Crum, S. Vaezy, *Ultrasound Med. Biol.* **31**, 1383 (2005). doi: [10.1016/j.ultrasmedbio.2005.06.004](https://doi.org/10.1016/j.ultrasmedbio.2005.06.004)
19. S. Howard, J. Yuen, P. Wegner, C. Zanelli, *IEEE Ultrasonics Symposium*, vol 2 p. 1270 (2003)
20. M.M. Doyley, J.C. Bamber, F. Fuechsel, N.L. Bush, *Ultrasound Med. Biol.* **27**, 1347 (2001). doi: [10.1016/S0301-5629\(01\)00429-X](https://doi.org/10.1016/S0301-5629(01)00429-X)
21. K.M. Quan, G.B. Christison, H.A. Mackenzie, P. Hodgson, *Phys. Med. Biol.* **38**, 1911 (1993). doi: [10.1088/0031-9155/38/12/014](https://doi.org/10.1088/0031-9155/38/12/014)
22. E.L. Madsen, G.R. Frank, F. Dong, *Ultrasound Med. Biol.* **24**, 535 (1998). doi: [10.1016/S0301-5629\(98\)00013-1](https://doi.org/10.1016/S0301-5629(98)00013-1)
23. K. Matre, A.B. Ahmed, H. Gregersen, A. Heimdal, T. Hausken, S. Odegaard, O.H. Gilja, *Ultrasound Med. Biol.* **29**, 1725 (2003). doi: [10.1016/j.ultrasmedbio.2003.08.006](https://doi.org/10.1016/j.ultrasmedbio.2003.08.006)
24. N. Maikusa, T. Fukami, T. Yuasa, Y. Tamura, T. Akatsuka, *J. Acoust. Soc. Am.* **122**, 672 (2007). doi: [10.1121/1.2743160](https://doi.org/10.1121/1.2743160)
25. F. Forsberg, W.T. Shi, M.K. Knauer, A.L. Hall, C. Vecchio, R. Bernardi, *Ultrason. Imaging* **27**, 65 (2005)
26. M. Bazzocchi, *Ecografia*, 2nd edn. (Idelson Gnocchi, Naples, 2001)
27. S. Casciaro, C. Demitri, R. Palmizio Errico, F. Conversano, G. Palma, E. Casciaro, A. Distante, *IEEE Ultrasonics Symposium*, vol 3 p. 1668 (2005)
28. L. Filipczynski, J. Wojcik, T. Kujawska, G. Lypacewicz, R. Tymkiewicz, B. Zienkiewicz, *Ultrasound Med. Biol.* **27**, 251 (2001). doi: [10.1016/S0301-5629\(00\)00329-X](https://doi.org/10.1016/S0301-5629(00)00329-X)
29. W.R. Hedrick, D.L. Hykes, D.E. Starchman, *Ultrasound Physics and Instrumentation*, 3rd edn. (Mosby, St. Louis, 1995)